# On the importance of anandamide structural features for its interactions with DPPC bilayers: effects on $PLA_2$ activity

**S. Ambrosi,* L. Ragni,† A. Ambrosini,* L. Paccamiccio,§ P. Mariani,§ R. Fiorini,* E. Bertoli,* and G. Zolese[1,*]**

Istituto di Biochimica* and Istituto di Scienze Fisiche,§ Università Politecnica delle Marche, 60131 Ancona, Italy; and Dipartimento di Biologia Molecolare, Cellulare, Animale (MCA),† Università di Camerino, 62032 Camerino, Italy

**Abstract The acylethanolamide anandamide (AEA) occurs in a variety of mammalian tissues and, as a result of its action on cannabinoid receptors, exhibits several cannabimimetic activities. Moreover, some of its effects are mediated through interaction with an ion channel-type vanilloid receptor. However, the chemical features of AEA suggest that some of its biological effects could be related to physical interactions with the lipidic part of the membrane. The present work studies the effect of AEA-induced structural modifications of the dipalmitoylphosphatidylcholine (DPPC) bilayer on phospholipase $A_2$ ($PLA_2$) activity, which is strictly dependent on lipid bilayer features. This study, performed by 2-dimethylamino-(6-lauroyl)-naphthalene fluorescence, demonstrates that the effect of AEA on $PLA_2$ activity is concentration-dependent. In fact, at low AEA/DPPC molar ratios (from $R = 0.001$ to $R = 0.04$), there is an increase of the enzymatic activity, which is completely inhibited for $R = 0.1$. X-ray diffraction data indicate that the AEA affects DPPC membrane structural properties in a concentration-dependent manner. Because the biphasic effect of increasing AEA concentrations on $PLA_2$ activity is related to the induced modifications of membrane bilayer structural properties, we suggest that AEA-phospholipid interactions may be important to produce, at least in part, some of the similarly biphasic responses of some physiological activities to increasing concentrations of AEA.**—Ambrosi, S., L. Ragni, A. Ambrosini, L. Paccamiccio, P. Mariani, R. Fiorini, E. Bertoli, and G. Zolese. **On the importance of anandamide structural features for its interactions with DPPC bilayers: effects on $PLA_2$ activity. *J. Lipid Res.* 2005.** 46: **1953–1961.**

**Supplementary key words** dipalmitoylphosphatidylcholine • Laurdan • X-ray diffraction • phospholipase $A_2$

Acylethanolamides (*N*-acylethanolamines; NAEs) are a class of naturally occurring single-chain membrane lipids that are widely distributed in plant, invertebrate, and mammalian tissues (1). They also accumulate in many organs under a large variety of pathological conditions (2), such as in brain during neurodegeneration (3) and in cerebrospinal fluid of schizophrenic patients (4). The NAE anandamide (arachidonoylethanolamide; AEA) occurs in a variety of mammalian tissues and, as a result of its action on cannabinoid receptors, exhibits several cannabimimetic activities (5). Moreover, some of its effects are mediated through an interaction with an ion channel-type vanilloid receptor (6).

AEA presents interesting pharmacological actions in many different tissues (7–12). On the other hand, NAEs, with saturated and monounsaturated acyl chains, present some biological activities but are thought to be inactive towards cannabinoid (CB) receptors (13, 14). The chemical nature of these NAEs and experimental evidence (15–19) suggest that some of their biological effects could be related, at least in part, to physical interactions with the lipidic part of the membrane. Because AEA is a largely hydrophobic molecule, it is possible that its local concentration in close proximity to the cannabinoid receptor binding site, which is localized within the lipid bilayer (20), may be considerably higher than that in aqueous environments outside the cells (21). Therefore, it is reasonable to suppose that AEA binding to CB receptors can be modulated by the physical and structural properties of the lipid bilayer and/or by AEA effects on the lipidic part of the membrane. Furthermore, the possible AEA-induced

*Manuscript received 31 March 2005 and in revised form 31 May 2005.*

*Published, JLR Papers in Press, June 16, 2005.*
*DOI 10.1194/jlr.M500121-JLR200*

Abbreviations: AEA, anandamide; *d*, unit cell dimension; DPPC, dipalmitoylphosphatidylcholine; emGP, emission generalized polarization; exGP, excitation generalized polarization; GP, generalized polarization; Laurdan, 2-dimethylamino-(6-lauroyl)-naphthalene; LUV, large unilamellar vesicle; MLV, multilamellar vesicle; NAE, acylethanolamide; PL, phospholipid; $PLA_2$, phospholipase $A_2$; $\tau$, lag time; Tm, main phase transition temperature.

[1] To whom correspondence should be addressed.
e-mail: g.zolese@univpm.it

physicochemical and/or structural modifications of the lipidic part of the membrane likely affect other important membrane physiological functions, which are known to be modulated by lipid bilayer properties, such as enzymatic activities, membrane permeability, hormonal response, etc. (18 and references cited therein).

In previous work, we studied the effect of NAEs with saturated and monounsaturated acyl chains on the physicochemical and structural properties of liposomal membranes of dipalmitoylphosphatidylcholine (DPPC) and egg phosphatidylethanolamine (16, 17). Moreover, we demonstrated that saturated and monounsaturated NAEs affect the activity of a secretory phospholipase $A_2$ (18) that is largely dependent on the structural, physicochemical, and dynamic properties of the lipid bilayer (22–24). Secretory $PLA_2$s are a family of water-soluble enzymes (13–15 kDa) that are structurally and mechanistically related. These proteins catalyze the hydrolysis of the *sn*-2 ester bond of glycerophospholipids and are involved in lipid metabolism and transduction pathways. There is increasing evidence of the important role of secretory $PLA_2$ in many physiological pathways, such as immune events, allergic reactions, spermatozoa acrosomal reaction, etc. Moreover, increased levels of secretory $PLA_2$ have been reported in inflammatory tissues (25) and in several tumor types (26). We demonstrated that the acyl chain length and/or the presence of a single double bond was crucial both for the NAE interaction with the lipid bilayer and for the effect exerted on enzymatic activity (18).

The aim of this work was to investigate the effect of AEA on $PLA_2$ activity and on the structural and physicochemical properties of lipid bilayers. In fact, the evaluation of AEA-bilayer interactions and their effects on $PLA_2$ activity could help in understanding, at least in part, the molecular reasons for the different physiological and pharmacological roles of NAEs with different acyl chains. DPPC large unilamellar vesicles (LUVs) were used for these studies to compare our results with recent reports on $PLA_2$ activity modulation by the lipid surface and with our previous work with saturated and monounsaturated NAEs (18).

In fact, because many details of the enzymatic activity have been clarified in liposomes (e.g., the temperature dependence of the enzymatic rate), these systems are largely used as fairly simple model systems to investigate the interplay between $PLA_2$ activity and the physicochemical features of lipid bilayers (27, 28).

## MATERIALS AND METHODS

The fluorescent probe 2-dimethylamino-(6-lauroyl)-naphthalene (Laurdan) was purchased from Molecular Probes (Eugene, OR). DPPC was obtained from Avanti Polar Lipids (Alabaster, AL). AEA was purchased from Sigma (St. Louis, MO).

Porcine pancreas $PLA_2$ (Sigma) was dialyzed in water, lyophilized, and stored at −20°C. Stock solutions of DPPC and Laurdan, dissolved in chloroform, were stored at −20°C. AEA was dissolved in ethanol immediately before use. The buffer used was 10 mM HEPES, 0.12 M NaCl, 50 mM KCl, and 1 mM EGTA (pH 7.4).

### Fluorescence measurements

DPPC and Laurdan solutions were mixed to a final probe-lipid phosphate molar ratio of 1:1,000. The solvent was then removed at room temperature under a nitrogen stream, and the sample was lyophilized for several hours in the dark. DPPC LUVs were prepared by extrusion through 0.1 μm polycarbonate filters 25 times at 55°C using the apparatus LiposoFast, as described previously (23). LUVs were diluted to a final concentration of 0.3 mM lipid phosphate; $PLA_2$ was 0.5 μM. When present, AEA in ethanol was added to LUVs at different molar ratios. Because AEA was always dissolved in 1 μl of ethanol, control experiments were performed with the same volume of this solvent; no significant effects of ethanol DPPC physicochemical properties on $PLA_2$ activity were measured (data not shown). Hydrolysis was triggered by 5 mM $Ca^{2+}$ injection in the cuvette containing liposomes and the enzyme at a final volume of 2 ml. Data were acquired at 38.6°C. Laurdan steady-state fluorescence measurements were performed on a Perkin-Elmer LS50 B. The fluorescent probe Laurdan is located at the hydrophobic-hydrophilic interface of the bilayer (at the glycerol backbone) (29). Its spectral features are largely sensitive to the polarity and to the molecular dynamics of solvent dipoles in the probe microenvironment (29, 30). Because these parameters are very different in the gel and in the liquid-crystalline phases of phospholipids (PLs), this probe was used to monitor PL phase changes (29, 30). Below the main phase transition temperature (Tm; i.e., in the gel phase), the Laurdan emission maximum is near 440 nm, whereas above the Tm (i.e., in the liquid-crystalline phase), this maximum is shifted to 490 nm (30). The excitation generalized polarization (exGP) measured at $\lambda_{exc}$ = 340 nm ($exGP^{340}$) (calculated on emission spectra obtained by $\lambda_{ex}$ = 340 nm) quantitatively relates the relative fluorescence intensities at 440 and 490 nm. These values were demonstrated to be independent of PL head groups and pH changes (in the range $4 < pH < 10$). The $exGP^{340}$ values measured in PL undergoing phase changes (28, 29) or in liposomes of different composition (31) have been related to the number and motional freedom of water molecules in the probe microenvironment. $ExGP^{340}$ was used as an index of the hydration level (polarity) of the lipid bilayer (31), in the region of the head groups at the hydrophobic-hydrophilic interface. Moreover, it was a useful probe to monitor $PLA_2$ hydrolytic activity (18).

Laurdan $exGP^{340}$ was calculated from Laurdan emission spectra ($\lambda_{exc}$ = 340 nm) by the following equation (29, 30):

$$GP = (I_B - I_R)/(I_B + I_R)$$

where $I_B$ and $I_R$ are, respectively, the intensity at 440 and 490 nm. An $exGP^{340}$ decrease represents an increase of bilayer polarity.

$ExGP^{340}$ cannot be used as a final proof of the coexistence of separate PL phase domains (31). However, it was demonstrated that the generalized polarization (GP) behavior, as a function of excitation and emission wavelengths, is sensitive to phase coexistence in lipid systems (31). Emission generalized polarization (emGP) spectra were obtained by calculating the GP value for each emission wavelength by the following formula (32):

$$emGP = (I_{410} - I_{340})/(I_{410} + I_{340})$$

where $I_{410}$ and $I_{340}$ are the intensities measured at each emission wavelength. These values are obtained by fluorescence emission spectra recorded at fixed excitation wavelengths of 410 and 340 nm, respectively.

ExGP spectra were obtained by calculating the GP value for each excitation wavelength using the following formula (32):

$$exGP = (I_{440} - I_{490})/(I_{440} + I_{490})$$

where $I_{440}$ and $I_{490}$ are the intensities measured at each excitation wavelength. These values are obtained by fluorescence exci-

tation spectra recorded at fixed emission wavelengths of 440 and 490 nm, respectively. The choice of 410, 340, 440, or 490 nm for GP calculation was based on the characteristic excitation and emission wavelengths of pure gel and liquid-crystalline lipid phases (31). The emGP and exGP spectra show characteristic patterns in the presence of pure or coexisting lipid phases (32).

### X-ray diffraction

Samples for X-ray diffraction were prepared as follows. AEA and DPPC were combined in the appropriate amounts in chloroform solutions and dried under a dry nitrogen stream to obtain a homogeneous film on a glass tube. The tube was left under vacuum for several hours to remove all traces of the organic solvent. The lipid film was hydrated by adding an excess of the same buffer used for fluorescence measurements; to obtain the homogeneous mixture, hydrated samples were subjected to heat shock cycles and then left for 1 day at 4°C in the dark. In these condition, X-ray diffraction spectra were found to be time-independent for periods of 1–2 weeks. The analyzed AEA-DPPC molar ratios ($R$) were 0, 0.02, and 0.2.

X-ray diffraction experiments were performed using a 3.5 kW PW 1830 X-ray generator (Philips, Eindhoven, The Netherlands) equipped with a Guinier-type focusing camera (Inel, Artenay, France) operating with a bent quartz crystal monochromator ($\lambda$ = 0.154 nm). Diffraction patterns were recorded on an Inel CPS 120 detector. Samples were held in a vacuum-tight cylindrical cell provided with thin Mylar windows. Diffraction data were collected at different temperatures (20, 34.5, 38.8, 40.5, and 50°C). The temperature was controlled using a Haake F3 thermostat (ThermoHaake, Karlsruhe, Germany) with an accuracy of 0.1°C. Before each measurement, the sample was maintained at the requested temperature for at least 10 min.

In each experiment, a number of Bragg peaks (at least three) were observed in the low-angle X-ray diffraction region, and their spacings were measured. The peak indexing was performed considering the different symmetries commonly observed in lipid phases (33, 34). The indexing problem was easy to solve, because at all of the different conditions of temperature and composition investigated, the spacing ratios of the observed Bragg peaks were fully compatible with the one-dimensional lamellar symmetry (spacing ratios 1:2:3...). From the averaged spacing of the observed peaks, the unit cell dimension ($d$), which corresponds to the distance between the midplane of two opposing lipid bilayers, was finally calculated. The nature of the short-range lipid conformation was derived by analyzing the high-angle X-ray diffraction profiles. In fact, it is well known that the high-angle pattern is characteristic of the lipid chain organization. A very sharp peak superposed to a rather broad reflection is detected when the hydrocarbon chains, rigid, fully extended, and tilted with respect to the lamellar plane, are packed in a distorted hexagonal structure [the lamellar phase is known as the gel phase ($L\beta'$)]. By contrast, a narrow diffraction peak is observed when the chains are rigid, fully extended, and packed in a hexagonal array [this phase is known as the ripple phase ($P\beta'$)]. Finally, a broad and flat diffraction peak reflects the liquid-like conformation of the hydrocarbon chains [this phase is known as the liquid-crystalline phase ($L\alpha$)]. In the present experimental conditions, all three different characteristic profiles were detected.

It should be observed that in pure DPPC in fully hydrated conditions, temperature induces the transition between the different phases: the first phase transition, which corresponds to the transition from the $L\beta'$ to the $P\beta'$ phase and that occurs at ~35°C, is known as pretransition, whereas the second transition, related to the melting of the hydrocarbon chain occurring at ~42°C and then to the transition from the $P\beta'$ to the $L\alpha$ phase, is named the main transition.

## RESULTS

### Effects of increasing concentrations of AEA on DPPC phase behavior: fluorescence measurements

The AEA concentrations used in this study were 0.3, 3, 4, 6, 12, and 30 μM, corresponding to AEA/DPPC molar ratios ($R$) of 0.001, 0.01, 0.013, 0.02, 0.04, and 0.1, respectively.

The thermotropic behavior of Laurdan $exGP^{340}$ was measured in DPPC LUVs (**Fig. 1**). Previous studies demonstrated that DPPC LUVs and multilamellar vesicles (MLVs) have nearly identical phase behavior, with similar pretransition and main transition temperatures (35), and the gel-to-liquid-crystalline phase transition of DPPC LUVs is known to be highly cooperative (18, 36 and references cited therein). In agreement with previous data (18, 29), Laurdan $exGP^{340}$ values (Fig. 1) show a large decrease at the main phase transition of DPPC LUV, whereas it is very difficult to assess the presence of the pretransition by the small slope changes shown by GP curves, although they occur at a temperature (~36.5°C) similar to previously reported data. For this reason, only the gel-to-liquid-crystalline phase transition will be discussed for all samples. Figure 1 shows that 0.3 μM AEA ($R$ = 0.001) does not largely affect the Tm and the width of the gel-to-liquid-crystalline phase transition. These data suggest that there is no lateral phase separation in lipid domains with different lipid composition within the bilayer, although the presence of small-scale microheterogeneity with clusters of different lipid composition cannot be excluded. The larger AEA concentrations (from 3 to 30 μM) ($0.01 \leq R \leq 0.1$) decrease DPPC Tm and broaden the tempera-

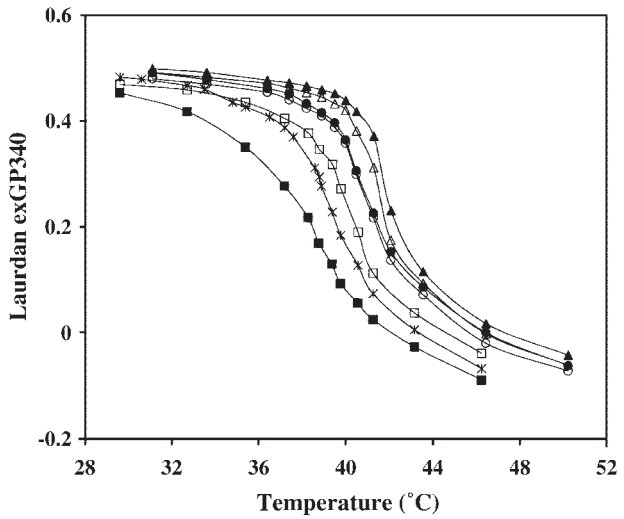


**Fig. 1.** Effect of increasing concentrations of anandamide (AEA) on 2-dimethylamino-(6-lauroyl)-naphthalene (Laurdan) excitation generalized polarization (exGP; $\lambda_{ex}$ = 340 nm) measured in dipalmitoylphosphatidylcholine (DPPC) large unilamellar vesicles (LUVs) as a function of temperature. Closed triangles, control. AEA/DPPC molar ratios ($R$) are as follows: open triangles, $R$ = 0.001; open circles, $R$ = 0.010; closed circles, $R$ = 0.013; open squares, $R$ = 0.020; asterisks, $R$ = 0.040; closed squares, $R$ = 0.10.

ture transition range, suggesting the presence of domains of different lipid composition.

**Table 1** shows the effect of increasing concentrations of AEA on Laurdan exGP$^{340}$ measured at 38.6°C both in the absence and the presence of $PLA_2$. All data were acquired in the absence of $Ca^{2+}$. Results obtained show that AEA at 3 μM ($R \geq 0.01$) significantly increases the bilayer hydration (bilayer polarity) measured in the probe microenvironment. Table 1 also reports exGP$^{340}$ values calculated in each lipid mixture after incubation with $PLA_2$ but in the absence of $Ca^{2+}$. The results obtained indicate that the enzyme does not significantly perturb the Laurdan microenvironment, either in the absence or the presence of AEA, as indicated by unmodified values of exGP$^{340}$ (Table 1).

**Figure 2** shows the wavelength dependence of exGP and emGP spectra in DPPC LUVs at 38.6°C in the absence and presence of AEA. The wavelength dependence of the GP pattern in these samples changes gradually, always showing a slight positive slope for exGP and a negative slope for emGP, although this is slightly more evident in samples containing AEA. This spectral slope is characteristic of gel/liquid-crystalline phase coexistence (32) and is evident both for pure DPPC and for each AEA concentration shown in the figure. A similar behavior is also seen at lower AEA concentrations (data not shown). The pattern of the wavelength dependence of exGP and emGP spectra, together with their shift to lower GP values with increasing AEA concentrations, are likely to be related to an AEA-induced increase of bilayer microheterogeneity. From Figs. 1, 2 and by X-ray studies (see below), we conclude that at the temperature used to measure $PLA_2$ activity, all samples tested in this work are in the gel phase or in the range of phase transition but not in the liquid-crystalline phase.

### Effects of increasing concentrations of AEA on DPPC phase behavior: X-ray diffraction measurements

X-ray diffraction experiments were performed on DPPC MLVs prepared in the absence or presence of AEA. It should be observed that DPPC MLVs can be compared with DPPC LUVs, because their thermal behavior is similar. In particular, it has been shown that both DPPC MLV and DPPV LUV display two transitions at similar temperatures (35, 37). It is well known that in DPPC MLV, these temperatures correspond to gel-to-ripple and to ripple-to-liquid-crystalline phase transitions, respectively, and it has been demonstrated that the corresponding transitions in DPPC LUV give rise to the same lipid phases (38).

TABLE 1. Effect of increasing concentrations of AEA on 2-dimethylamino-(6-lauroyl)-naphthalene exGP$^{340}$ in the absence and presence of $PLA_2$

| AEA | AEA/DPPC Molar Ratio | No $PLA_2$ | With $PLA_2$ |
|---|---|---|---|
| *μM* | *R* | | |
| 0 | 0 | 0.441 ± 0.017 (9) | 0.440 ± 0.010 (6) |
| 0.3 | 0.001 | 0.444 ± 0.016 (3) | 0.451 ± 0.006 (3) |
| 3 | 0.010 | 0.391 ± 0.027[a] (4) | 0.402 ± 0.006[b] (3) |
| 4 | 0.013 | 0.395 ± 0.024[c] (3) | 0.409 ± 0.012[a] (3) |
| 6 | 0.020 | 0.365 ± 0.021[b] (3) | 0.364 ± 0.010[b] (3) |
| 12 | 0.040 | 0.315 ± 0.040[b] (4) | 0.304 ± 0.006[b] (3) |
| 30 | 0.100 | 0.178 ± 0.046[b] (3) | 0.139 ± 0.034[b] (3) |

AEA, anandamide; DPPC, dipalmitoylphosphatidylcholine; $PLA_2$, phospholipase $A_2$. Numbers in parentheses represents the number of experiments performed for each sample. Significance was tested by Student's *t*-test.

[a] $P < 0.010$ control versus sample measured in the same conditions.

[b] $P < 0.001$ control versus sample measured in the same conditions.

[c] $P < 0.05$ control versus sample measured in the same conditions.

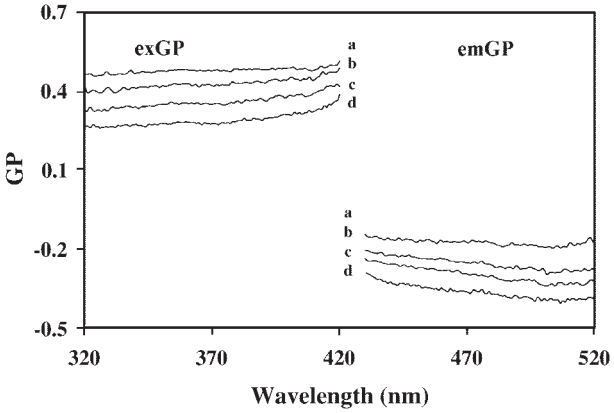


**Fig. 2.** ExGP and emGP spectra recorded in DPPC LUVs as a function of increasing AEA/DPPC molar ratios: trace a, control; trace b, $R = 0.02$; trace c, $R = 0.04$; trace d, $R = 0.1$. Temperature = 38.6°C.

The AEA/DPPC molar ratios considered were 0, 0.02, 0.1, and 0.2, and measurements were performed at different temperatures, from 20°C to 50°C (i.e., temperatures at which pure DPPC samples occur as gel, ripple, and liquid-crystalline phases). The main purpose of these measurements was to determine whether the presence of increasing concentrations of AEA can induce transitions from the lamellar to the nonlamellar phase, as suggested by the large acyl chain unsaturation of AEA, which is expected to modulate the curvature of the polar-apolar interface and then to affect the polymorphic phase behavior of membrane lipids [$H_{II}$ phase is reviewed by Hafez and Cullis (39)]. Moreover, X-ray experiments were used to assess the possible presence of phase separation, even if only large multiphase domains are usually revealed.

Low- and high-angle diffraction patterns (**Figs. 3**, **4**, respectively) were analyzed separately. Phase structures and *d* values were derived from low-angle diffraction data, whereas high-angle data were used to determine the hydrocarbon chain conformations.

As a first notable result, it can be observed that at all of the considered temperatures and AEA concentrations, the spacing of the low-angle diffraction peaks was unambiguously indexed according to a lamellar one-dimensional symmetry: at all the investigated experimental conditions, samples form lamellar structures, which occur as single phases. However, the high-angle diffraction profiles indicate that the lipid hydrocarbon chain conformation depends on sample composition. As expected, in fully hydrated DPPC systems, three different lamellar phases are formed as a function of temperature: the Lβ′, Pβ′, and Lα

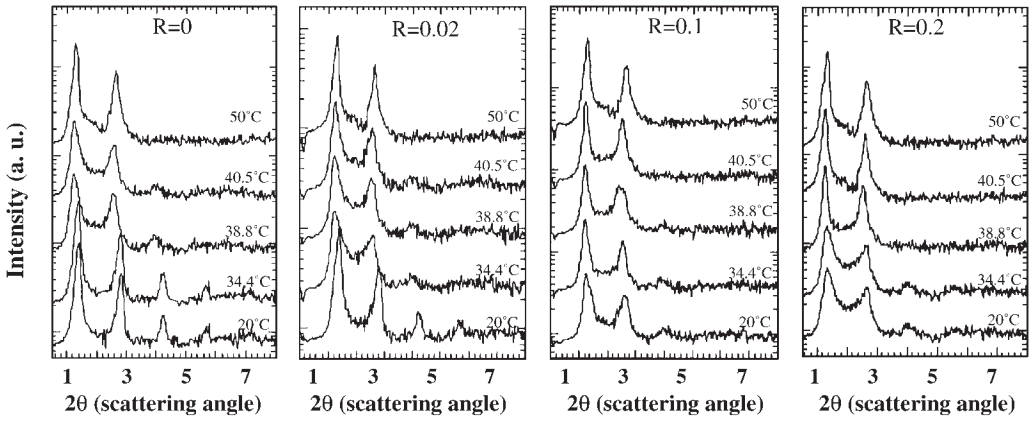


**Fig. 3.** Low-angle X-ray diffraction profiles obtained for fully hydrated DPPC multilamellar vesicles (MLVs) prepared in the absence and presence of AEA at AEA/DPPC molar ratios of 0, 0.02, 0.1, and 0.2. Each experiment was performed at 38.8°C. Scattering intensitites are reported in arbitrary units (a.u.) as a function of the scattering angle 2θ.

phases. Moreover, a similar phase behavior is detected in the sample prepared at the lower AEA concentration ($R$ = 0.02). On the contrary, samples with AEA/DPPC $R$ = 0.1 and $R$ = 0.2 clearly show that the ripple phase already forms at 20°C. Moreover, in these samples, the main transition is detected to occur at a temperature a few degrees lower than in pure DPPC.

From the position of the peaks observed in the low-angle scattering region, the $d$ values were determined as a function of the different experimental conditions: the dependence on temperature observed in the different investigated samples is reported in **Table 2**. In pure DPPC samples in excess water, the behavior is in agreement with previous results (40). In the Lβ phase, the unit cell increases as a function of temperature (6.29 and 6.48 nm at 20°C and 34.4°C, respectively; Table 2) because of the thermal dependence of the chain-tilting angle; in the Pβ′ phase, the $d$ is constant and rather large, because of the formation of periodic ripples (usually with periods in the range of 100–300 Å), which increases the intensity of the repulsive steric forces between the membranes (35, 40) (Table 2). The range of existence of the Pβ′ phase is very small, so that the $d$ appears practically independent on temperature (7.12 and 7.13 nm at 38.8°C and 40.5°C, respectively; Table 2). At the main transition, the lipid hydrocarbon chains assume a liquid-like conformation, and a large reduction of the unit cell distance is detected. Because of the decrease of the chain order parameter, the unit cell in Lα is reduced further as a function of temperature (6.69 nm at 50°C; Table 2). It should be noted that below the pretransition and above the main transition, the membrane is planar.

A similar behavior is observed at a low AEA molar ratio ($R$ = 0.02), even if data at 34.4°C indicate that the pretransition is anticipated (the Pβ′ phase is already formed at this temperature) (Table 2). The shift of pretransition to lower temperatures is also confirmed by results obtained at the higher AEA concentration analyzed. In particular, the main effect detected at 20°C in the $R$ = 0.1 and $R$ = 0.2 samples is a shift of the low-angle reflections to

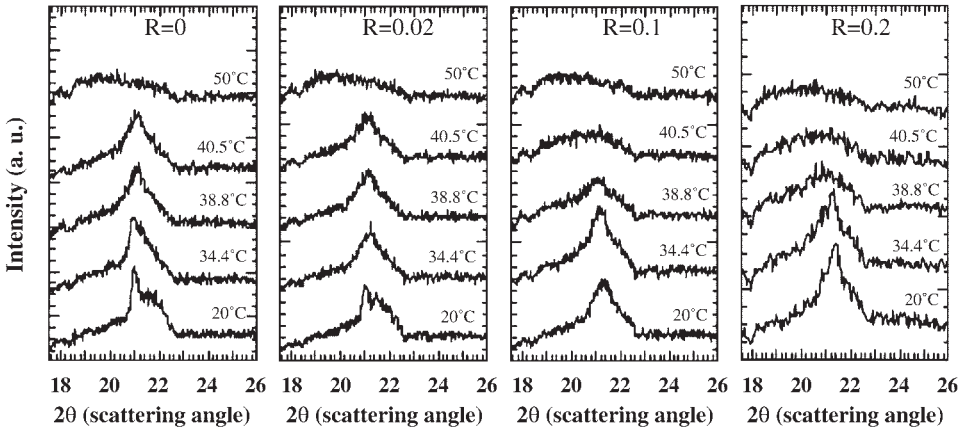


**Fig. 4.** High-angle X-ray diffraction profiles obtained for fully hydrated DPPC MLVs prepared in the absence and presence of AEA at AEA/DPPC molar ratios of 0, 0.02, 0.1, and 0.2. Each experiment was performed at 38.8°C. Scattering intensitites are reported in arbitrary units (a.u.) as a function of the scattering angle 2θ.

TABLE 2. X-ray diffraction data in DPPC liposomes containing increasing AEA/DPPC molar ratios

| Temperature | Phase | Unit Cell Dimension |
|---|---|---|
| °C | | Å |
| Pure DPPC | | |
| 20 | Lβ′ | 62.90 |
| 34.4 | Lβ′ | 64.75 |
| 38.8 | ripple | 71.20 |
| 40.5 | ripple | 71.30 |
| 50 | Lα | 66.85 |
| $R = 0.02$ | | |
| 20 | Lβ′ | 63.45 |
| 34.4 | ripple | 68.95 |
| 38.8 | ripple | 71.45 |
| 40.5 | ripple | 71.50 |
| 50 | Lα | 67.11 |
| $R = 0.1$ | | |
| 20 | ripple | 67.40 |
| 34.4 | ripple | 70.85 |
| 38.8 | ripple | 73.60 |
| 40.5 | Lα | 71.78 |
| 50 | Lα | 67.59 |
| $R = 0.2$ | | |
| 20 | ripple | 65.96 |
| 34.4 | ripple | 67.25 |
| 38.8 | Lα | 70.19 |
| 40.5 | Lα | 69.30 |
| 50 | Lα | 67.20 |

Lα, liquid-crystalline phase; Lβ′, gel phase.

lower 2θ angles (scattering angles), which corresponds to an increase of lamellar repeat spacing to 6.74 nm in the $R = 0.1$ sample and a subsequent decrease to 6.60 nm in the $R = 0.2$ sample (compared with the value of 6.29 nm measured on DPPC at 20°C; Table 2) and a broadening of the diffraction peaks. According to the high-angle profiles, this behavior confirms that AEA shifts the appearance of the ripple phase to lower temperatures, even if the dependence of lamellar repeat spacing from the AEA concentration is rather surprising. This special feature characterizes all samples showing the ripple structure: the periodicity increases as a function of the AEA concentration but then decreases at the higher investigated molar ratio ($R = 0.2$; Table 2). Furthermore, upon heating, the lamellar *d* spacing values of the $R = 0.2$ sample increase from 6.73 nm in the ripple phase at 34.4°C to 7.02 ± 0.29 nm in the Lα phase at 38.8°C (Table 2). No similar behavior is evident in the other AEA/DPPC samples. Also notable is the fact that at 50°C (i.e., when all samples are in the liquid-crystalline phase), *d* values show no differences at any of the investigated AEA concentrations.

### Effect of increasing concentrations of AEA on $PLA_2$ activity

In the presence of zwitterionic PL vesicles, $PLA_2$ activity is characterized by a latency period [identified as lag time (τ)] of slow rate followed by an abrupt increase of the hydrolytic rate. This increase of enzymatic rate at the τ is believed to be dependent on the formation of threshold concentrations of the reaction products. The length of the τ is dependent on various factors, such as structure, composition, and lipid lateral segregation into domains. The increase of $PLA_2$ activity near the lipid Tm was related to the increase of the heterogeneous lateral bilayer structure (41) caused by thermal density fluctuations. In this work, $PLA_2$ activity studies were performed on DPPC LUVs at a temperature (38.6°C) below the main PL transition (41.5°C for DPPC LUVs in our experimental conditions) to compare data with a previous study performed, in similar conditions, with saturated and monounsaturated NAEs. The fluorescent features of Laurdan were used to study enzymatic activity, according to a previous work (18). Briefly, the time-dependent change of Laurdan $exGP^{340}$ data was monitored after the addition of 5 mM $Ca^{2+}$ to DPPC LUVs (18). It was shown that, in these conditions, Laurdan $exGP^{340}$ exhibits an abrupt decrease that is coincident with the increase of enzymatic activity at the τ (18). The time course of vesicle hydrolysis in DPPC LUVs showed that AEA induces the decrease of τ at all concentrations tested except for 30 μM AEA (**Table 3**). In fact, no enzymatic activity is measured at this AEA concentration, whereas the maximum activity (measured as the larger decrease of τ) is obtained at 6 μM AEA (−49.7% compared with pure DPPC; Table 3).

## DISCUSSION

It was demonstrated that $PLA_2$ hydrolytic activity is significantly affected by the presence of lipid lateral segregation into domains and by other bilayer defects, which can be in the form of holes in the bilayer (42, 43) or line defects occurring in bilayers undergoing density fluctuations near the Tm (41). In fact, the increase of $PLA_2$ activity near the lipid Tm was related to the contemporary increase of the heterogeneous lateral bilayer structure (41) caused by thermal density fluctuations. The degree of bilayer heterogeneity can be quantified as the amount of bilayer area occupied at the interfaces between the gel and fluid domains (44).

In general, temperature effects and other factors (such as the presence of exogenous molecules) that allow an easier access of the enzyme to substrate are thought to shift the reaction equilibrium toward the products. On the contrary, the rate of lipid hydrolysis is reduced by factors that modify bilayer physical properties in a way that promotes the desorption of bound enzyme. Furthermore,

TABLE 3. Effect of increasing concentrations of AEA on $PLA_2$ activity τ at 38.6°C

| AEA | τ | Percent Change |
|---|---|---|
| μM | min | |
| 0 | 37.8 ± 7.2 (6) | |
| 0.3 | 40.0 ± 0.1 (3) | +5.8 |
| 3.0 | 28.0 ± 2.8 (3) | −23.8 |
| 4.0 | 22.0 ± 4.2[a] (3) | −41.8 |
| 6.0 | 19.0 ± 2.8[b] (3) | −49.7 |
| 12.0 | 24.5 ± 4.9[a] (3) | −35.2 |
| 30.0 | No activity | |

τ, lag time. Numbers in parentheses represent the number of experiments performed for each sample. Significance was tested by Student's *t*-test.

[a] $P < 0.05$.

[b] $P < 0.01$.

it was postulated that $PLA_2$ presents an increased sensitivity toward regions of high curvature, such as the Pβ′ phase (45). It was shown that the hydrolysis occurs within the ripple valleys, indicating that the high-curvature regions are susceptible to hydrolysis (45). Laurdan GP thermotropic behavior in DPPC LUVs indicated that AEA induces concentration-dependent shifts of the lipid Tm to lower temperatures, likely because of the presence of unsaturations, which decrease acyl chain packing, favoring the transition to a fluid liquid-crystalline phase. Moreover, it is evident that increased AEA concentrations cause the greater width of the main transition. This behavior and the pattern of Laurdan GP spectra at 38.6°C (Fig. 2) suggest an AEA-induced increase of lipid bilayer heterogeneity. These results indicate that, at the temperature chosen for the reaction, no sample is in a pure liquid-crystalline phase; rather, gel and liquid-crystalline phases always coexist, which is expected to increase with AEA concentration. For these reasons, a strong correlation between the AEA-induced decrease of DPPC Tm and an increase of $PLA_2$ activity (measured as a decrease of the τ) is expected. As predicted, the low AEA concentrations (from 3 to 12 μM; corresponding to $R$ ranging from 0.001 to 0.04) increase the $PLA_2$ activity (Table 3) as a consequence of an increased lateral heterogeneity. However, the effect of 30 μM AEA (corresponding to AEA/DPPC $R = 0.1$) was unexpected, because no $PLA_2$ activity was recorded in this sample. X-ray diffraction data indicate no evident AEA-induced structural changes of Pβ′ phase in the $R = 0.02$ sample at the temperature used for activity studies.

These results support the hypothesis of a correlation between the increased $PLA_2$ activity and the higher AEA-induced microheterogeneity. This microheterogeneity is not incompatible with the presence of a pure Pβ′ phase, according to a recent model for this poorly characterized phase (35). This model attempts to explain the local spontaneous curvature observed in the ripple phase by suggesting that curvature derives from the presence of linear arrays of fluid state molecules coexisting with gel phase lipids. Ripples are considered to be one-dimensional defects of fluid lipid molecules (35). The increased $PLA_2$ activity induced by AEA ⩽ 12 μM could be explained by the increased degree of small-scale lateral structures caused by dynamic gel/fluid domain formation. On the other hand, X-ray diffraction data indicate a characteristic behavior for the ripple phases formed by the AEA/DPPC $R = 0.1$ and $R = 0.2$ samples. A similar but more evident behavior was described for bilayers formed at low temperatures by DPPC codispersed with branched-chain phosphatidylcholine (at a concentration of >5%) (46). In those samples, the peak broadening of small-angle reflections is associated with an initial increase of lamellar repeat spacing ($a$) for mixtures with 10 mol% branched lipid and with a subsequent $a$ decrease for the 20 mol% sample. This behavior was explained by the formation of rippled bilayers with unusually large periodicities (up to 120 nm), which were identified as macroripples that are characterized by a symmetrical ripple (47). With increasing concentrations of the branched phosphatidylcholine, the relative proportion of bilayers showing the ripples is decreased, whereas flat membrane structure increases (46), thus explaining the decrease of the lamellar repeat spacing. The formation of alternative ripples (often referred to as macroripples) was observed previously in many lipid mixtures containing a phosphatidylcholine able to form pretransition ripples (commonly DPPC or dimyristoylphosphatidylcholine) (48).

Semmler, Meyer, and Quinn (46) suggested that the incorporation of a second molecule in a gel phase phosphatidylcholine bilayer causes the formation of a different lipid superstructure, which likely depends on the detailed molecular structure of the incorporated molecule. A previous structural model (18) suggested that two hydrogen bonds are formed by NAEs with PL head groups: the nitrogen atom of the amide interacts with the carbonyl group of the *sn*-2 acyl chain, whereas the hydroxyl group of NAE is hydrogen bonded with the phosphate group. Because of the bent structure of AEA (49) (likely a closed-hairpin structure, which can be favored for the steric constraints exerted by the rigid DPPC molecules in the gel phase), the quite stable dimer AEA-DPPC could simulate a branched-chain phosphatidylcholine, suggesting possible AEA-induced macroripple formation on DPPC bilayers at low temperatures. In fact, macroripple was without doubt associated with the change of chain volume while maintaining a similar head group volume (48): in the AEA-DPPC dimer, the DPPC head group volume cannot be appreciably modified by the small hydroxyl group of AEA, whereas the chain volume is largely increased by the presence of the bent arachidonoyl acyl chain of AEA. It was suggested that, for macroripple formation, a certain proportion of fluid chains must be present to allow the periodic tilting of the bilayer, with the localization of fluid lipid in the crests and valleys of the macroripples (46). The Laurdan GP results (indicating an AEA-induced decrease of DPPC Tm and the presence of coexisting gel and fluid domains in the lipid mixtures studied) are in agreement with these data, supporting the hypothesis that quite large concentrations AEA (AEA/DPPC $R = 0.1$ and $R = 0.2$) can induce a reorganization of the gel phase DPPC. On the other hand, the increased value of the lamellar spacing measured in the $R = 0.2$ sample upon the formation of Lα phase could be a consequence of the increased conformational disorder of the phosphatidylcholine acyl chains, which could affect AEA interaction with DPPC (e.g., the proper localization of the NAE within the bilayer) and hydrogen bond formation. Although the AEA/DPPC $R = 0.2$ bilayer modifications, occurring at the transition of the ripple phase to the Lα phase, require further characterization, we hypothesize that the increased DPPC conformational disorder modifies the PL shape, avoiding the proper AEA localization within the bilayer and shifting it to a different location perpendicular to the bilayer. At this large AEA concentration, this effect could significantly affect the lamellar repeat spacing measured by X-ray diffraction.

Because the length scale of the Pβ′ ripple of a phosphatidylcholine was suggested to be relevant to the length

scale of the enzyme (45), the possibility of an AEA-induced modification of the ripple profile could explain the complete inhibition of $PLA_2$ shown by the $R = 0.1$ sample. Although several factors can come into play to affect $PLA_2$ activity, a possibility exists that the ripple profile of the sample AEA/DPPC $R = 0.1$ could be modified, depending on the temperature and relative degree of coexisting gel-fluid domains, so that porcine pancreatic $PLA_2$ cannot properly interact with the ripple to have useful accessibility to the lipids. This possibility is also suggested by the known structural requirements of the secretory $PLA_2$, which must make critical and specific interactions along its i-face (which is the interface binding region of the protein with the bilayer) to reach its fully activated form on an interface (50, 51).

## Conclusions

AEA concentrations used in this work are not normally present in biological membranes (2), although the AEA/lipid molar ratio $R = 0.001$ could be reached in some conditions, such as in murine uterus (the calculation can be made assuming 20 μmol lipid phosphorous/g tissue) (2). However, it was suggested that the possible preferential localization of the hydrophobic AEA in specific membrane domains of different lipid composition could give rise to an increase of its local concentration (21). As a consequence, we suggest the possible formation of microenvironments with particular structural and physicochemical features, as hypothesized previously for other NAEs (18). Data shown in this work indicate that increasing concentrations of AEA affect the membrane physicochemical and structural properties of a phosphatidylcholine bilayer differently. Moreover, the biphasic effect of increasing AEA concentrations on $PLA_2$ activity is related to the induced modifications of membrane bilayer properties. Many reports have shown similarly biphasic responses of physiological activities to increasing AEA concentrations (21 and references cited therein). These findings might have different explanations, such as an agonist-induced allosteric modulation of cannabinoid receptors, a large receptor reserve, or a coupling of cannabinoid receptors to both $G_i$ and $G_s$ proteins (21). Although our present data were obtained in model lipid systems and require further investigations to be related to AEA effects on living cells, they suggest the possibility that AEA-PL interactions may be important to produce these biphasic effects. The fact that the ligand binding sites for cannabinoid receptors are within the lipid bilayer of biological membranes (20) could support this hypothesis.

This work was supported by a grant from Ministero dell'Istruzione, Università e Ricerca (MIUR) to G.Z.

## REFERENCES


1. Schuel, H., L. J. Burkman, J. Lippes, K. Crickard, E. Forester, D. Piomelli, and A. Giuffrida. 2002. N-Acylethanolamines in human reproductive fluids. *Chem. Phys. Lipids.* **121:** 211–227.
2. Hansen, H. S., B. Moesgaard, H. H. Hansen, and G. Petersen. 2000. N-Acylethanolamines and precursor phospholipids—relation to cell injury. *Chem. Phys. Lipids.* **108:** 135–150.
3. Hansen, H. H., C. Ikonomidou, P. Bittigau, S. H. Hansen, and H. S. Hansen. 2001. Accumulation of the anandamide precursor and other N-acylethanolamine phospholipids in infant rat models of in vivo necrotic and apoptotic neuronal death. *J. Neurochem.* **76:** 39–46.
4. Leweke, F. M., A. Giuffrida, U. Wurster, H. M. Emrich, and D. Piomelli. 1999. Elevated endogenous cannabinoids in schizophrenia. *Neuroreport.* **10:** 1665–1669.
5. Hillard, C. J., and W. B. Campbell. 1997. Biochemistry and pharmacology of arachidonylethanolamide, a putative endogenous cannabinoid. *J. Lipid Res.* **38:** 2383–2398.
6. Howlett, A. C., and S. Mukhopadhyay. 2000. Cellular signal transduction by anandamide and 2-arachidonoylglycerol. *Chem. Phys. Lipids.* **108:** 53–70.
7. Schmid, P. C., B. C. Paria, R. J. Krebsbach, H. H. Schmid, and S. K. Dey. 1997. Changes in anandamide levels in mouse uterus are associated with uterine receptivity for embryo implantation. *Proc. Natl. Acad. Sci. USA.* **94:** 4188–4192.
8. Maccarrone, M., M. DeFelici, F. G. Klinger, N. Battista, F. Fezza, E. Dainese, G. Siracusa, and A. Finazzi-Agrò. 2004. Mouse blastocysts release a lipid which activates anandamide hydrolase in intact uterus. *Mol. Hum. Reprod.* **10:** 215–221.
9. Parolaro, D., P. Massi, T. Rubino, and E. Monti. 2002. Endocannabinoids in the immune system and cancer. *Prostaglandins Leukot. Essent. Fatty Acids.* **66:** 319–332.
10. Freund, T. F., I. Katona, and D. Piomelli. 2003. Role of endogenous cannabinoids in synaptic signaling. *Physiol. Rev.* **83:** 1017–1066.
11. Randall, M. D., D. Harris, D. A. Kendall, and V. Ralevic. 2002. Cardiovascular effects of cannabinoids. *Pharmacol. Ther.* **95:** 191–202.
12. Pate, D. W., K. Jarvinen, A. Urtti, V. Mahadevan, and T. Jarvinen. 1998. Effect of the CB1 receptor antagonist, SR141716A, on cannabinoid-induced ocular hypotension in normotensive rabbits. *Life Sci.* **63:** 2181–2188.
13. De Petrocellis, L., D. Melck, T. Bisogno, and V. Di Marzo. 2000. Endocannabinoids and fatty acid amides in cancer, inflammation and related disorders. *Chem. Phys. Lipids.* **108:** 191–209.
14. Berdyshev, E. V., P. C. Schmid, R. J. Krebsbach, C. J. Hillard, C. Huang, N. Chen, Z. Dong, and H. H. O. Schmid. 2001. Cannabinoid-receptor-independent cell signalling by N-acylethanolamines. *Biochem. J.* **360:** 67–75.
15. Schmid, H. H. O., P. C. Schmid, and V. Natarajan. 1990. N-Acylated glycerophospholipids and their derivatives. *Prog. Lipid Res.* **29:** 1–43.
16. Ambrosini, A., E. Bertoli, P. Mariani, F. Tanfani, M. Wozniak, and G. Zolese. 1993. N-Acylethanolamines as membrane topological stress compromising agents. *Biochim. Biophys. Acta.* **1148:** 351–355.
17. Ambrosini, A., F. Tanfani, E. Bertoli, M. Wozniak, Z. Wypych, and G. Zolese. 1993. Effect of N-acylethanolamines with different acyl-chains on DPPC multilamellar liposomes. *Chem. Phys. Lipids.* **65:** 165–169.
18. Zolese, G., M. Wozniak, P. Mariani, L. Saturni, E. Bertoli, and A. Ambrosini. 2003. Different modulation of phospholipase $A_2$ activity by saturated and monounsaturated N-acylethanolamines. *J. Lipid Res.* **44:** 742–753.
19. Bloom, A. S., W. S. Edgemond, and J. C. Moldvan. 1997. Nonclassical and endogenous cannabinoids: effects on the ordering of brain membranes. *Neurochem. Res.* **22:** 563–568.
20. Makriyannis, A., and R. S. Rapaka. 1990. The molecular basis of cannabinoid activity. *Life Sci.* **47:** 2173–2184.
21. Schuel, H., L. J. Burkman, J. Lippes, K. Crickard, M. C. Mahony, A. Giuffrida, R. P. Picone, and A. Makriyannis. 2002. Evidence that anandamide-signaling regulates human sperm functions required for fertilization. *Mol. Reprod. Dev.* **63:** 376–387.
22. Jain, M. K., M. H. Gelb, J. Rogers, and O. G. Berg. 1995. Kinetic bases for interfacial catalysis by phospholipase A2. *Methods Enzymol.* **249:** 567–614.
23. Bell, J. D., and R. L. Biltonen. 1992. Molecular details of the activation of soluble phospholipase A2 on lipid bilayers. Comparison of computer simulations with experimental results. *J. Biol. Chem.* **267:** 11046–11056.
24. Bell, J. D., M. Burnside, J. A. Owen, M. L. Royall, and M. L. Baker. 1996. Relationships between bilayer structure and phospholipase A2 activity: interactions among temperature, diacylglycerol, lyso-

lecithin, palmitic acid, and dipalmitoylphosphatidylcholine. *Biochemistry.* **35:** 4945–4955.
25. Vermehren, C., T. Kielber, I. Hylander, T. H. Callisen, and K. Jørgensen. 1998. Increase in phospholipase A2 activity towards lipopolymer-containing liposomes. *Biochim. Biophys. Acta.* **1373:** 27–36.
26. Laye, J. P., and J. H. Gill. 2003. Phospholipase A2 expression in tumours: a target for therapeutic intervention? *Drug Discov. Today.* **8:** 710–716.
27. Burack, W. R., A. R. Dibble, M. M. Allietta, and R. L. Biltonen. 1997. Changes in vesicle morphology induced by lateral phase separation modulate phospholipase A2 activity. *Biochemistry.* **36:** 10551–10557.
28. Callisen, T. H., and Y. Talmon. 1998. Direct imaging by cryo-TEM shows membrane break-up by phospholipase A2 enzymatic activity. *Biochemistry.* **37:** 10987–10993.
29. Parasassi, T., G. De Stasio, G. Ravagnan, R. M. Rusch, and E. Gratton. 1991. Quantitation of lipid phases in phospholipid vesicles by the generalized polarization of Laurdan fluorescence. *Biophys. J.* **60:** 179–189.
30. Parasassi, T., G. De Stasio, A. D'Ubaldo, and E. Gratton. 1990. Phase fluctuation in phospholipid membranes revealed by Laurdan fluorescence. *Biophys. J.* **57:** 1179–1186.
31. Hirsch-Lerner, D., and Y. Barenholz. 1999. Hydration of lipoplexes commonly used in gene delivery: follow-up by Laurdan fluorescence changes and quantification by differential scanning calorimetry. *Biochim. Biophys. Acta.* **1461:** 47–57.
32. Parasassi, T., M. Loiero, M. Raimondi, G. Ravagnan, and E. Gratton. 1993. Absence of lipid gel-phase domains in seven mammalian cell lines and in four primary cell types. *Biochim. Biophys. Acta.* **1153:** 143–154.
33. Mariani, P., V. Luzzati, and H. Delacroix. 1988. Cubic phases of lipid-containing systems. Structure analysis and biological implications. *J. Mol. Biol.* **204:** 165–189.
34. Luzzati, V. 1968. X-ray diffraction studies of lipid-water systems. *In* Biological Membranes. D. Chapman and F. H. Wallah, editors. Academic Press, London. 71–123.
35. Heimburg, T. 2000. A model for the lipid pretransition: coupling of ripple formation with the chain-melting transition. *Biophys. J.* **78:** 1154–1165.
36. Høyrup, P., O. G. Mouritsen, and J. Jorgensen. 2001. Phospholipase A(2) activity towards vesicles of DPPC and DMPC-DSPC containing small amounts of SMPC. *Biochim. Biophys. Acta.* **1515:** 133–143.
37. Heimburg, T. 1998. Mechanical aspects of membrane thermodynamics. Estimation of the mechanical properties of lipid membranes close to the chain melting transition from calorimetry. *Biochim. Biophys. Acta.* **1415:** 147–162.
38. Mason, P. C., B. D. Gaulin, R. M. Epand, G. D. Wignall, and J. S. Lin. 1999. Small angle neutron scattering and calorimetric studies of large unilamellar vesicles of the phospholipid dipalmitoylphosphatidylcholine. *Phys. Rev. E.* **59:** 3361–3367.
39. Hafez, I. M., and P. R. Cullis. 2001. Roles of lipid polymorphism in intracellular delivery. *Adv. Drug Deliv. Rev.* **47:** 139–148.
40. Janiak, M. J., D. M. Small, and G. G. Shipley. 1976. Nature of the thermal pretransition of synthetic phospholipids: dimyristolyl- and dipalmitoyllecithin. *Biochemistry.* **15:** 4575–4580.
41. Hønger, T., K. Jørgensen, D. Stokes, R. L. Biltonen, and O. G. Mouritsen. 1997. Phospholipase A2 activity and physical properties of lipid-bilayer substrates. *Methods Enzymol.* **286:** 168–190.
42. Grandbois, M., H. Clausen-Schumann, and H. Gaub. 1998. Atomic force microscope imaging of phospholipid bilayer degradation by phospholipase $A_2$. *Biophys. J.* **74:** 2398–2404.
43. Nielsen, L. K., J. Risbo, T. H. Callisen, and T. Bjørnholm. 1999. Lag-burst kinetics in phospholipase $A_2$ hydrolysis of DPPC bilayers visualized by atomic force microscopy. *Biochim. Biophys. Acta.* **1420:** 266–271.
44. Hønger, T., K. Jorgensen, R. L. Biltonen, and O. G. Mouritsen. 1996. Systematic relationship between phospholipase A2 activity and dynamic lipid bilayer microheterogeneity. *Biochemistry.* **35:** 9003–9006.
45. Leidy, C., O. G. Mouritsen, K. Jorgensen, and G. H. Peters. 2004. Evolution of a rippled membrane during phospholipase A2 hydrolysis studied by time-resolved AFM. *Biophys. J.* **87:** 408–418.
46. Semmler, K., H. W. Meyer, and P. J. Quinn. 2000. The structure and thermotropic phase behavior of dipalmitoylphosphatidylcholine codispersed with a branched-chain phosphatidylcholine. *Biochim. Biophys. Acta.* **1509:** 385–396.
47. Cunningham, B. A., A-D. Brown, D. H. Wolfe, W. P. Williams, and A. Brain. 1998. Ripple phase formation in phosphatidylcholine: effect of acyl chain relative length, position, and unsaturation. *Phys. Rev. E.* **58:** 3662–3672.
48. Meyer, H. W., B. Dobner, and K. Semmler. 1996. Macroripple-structures induced by different branched-chain phosphatidylcholines in bilayers of dipalmitoylphosphatidylcholine. *Chem. Phys. Lipids.* **82:** 179–189.
49. Piomelli, D., M. Beltramo, S. Glasnapp, S. Y. Lin, A. Goutopoulos, X. Q. Xie, and A. Makriyannis. 1999. Structural determinants for recognition and translocation by the anandamide transporter. *Proc. Natl. Acad. Sci. USA.* **96:** 5802–5807.
50. Ramirez, F., and M. K. Jain. 1991. Phospholipase A2 at the bilayer interface. *Proteins.* **9:** 229–239.
51. Bahnson, B. J. 2005. Structure, function and interfacial allosterism in phospholipase A2: insight from the anion-assisted dimer. *Arch. Biochem. Biophys.* **433:** 96–106.